Computational Approach to Micromechanical Contacts

Lecture 6.
Contact of rough surfaces

Vladislav A. Yastrebov

MINES ParisTech, PSL Research University, Centre des Matériaux, CNRS UMR 7633, Evry, France

@ Centre des Matériaux
September 2017

Problem statement & methods

Problem

- Solve contact problem for two elastic half-spaces E_1, ν_1 and E_2, ν_2
- With surface roughnesses $z_1(x, y)$ and $z_2(x, y)$
- Balance of momentum $\nabla \cdot \underline{\underline{\sigma}} = 0$,
- Boundary conditions $-\sigma_z^\infty = p_0$
- Contact constraints $g \geq 0, \quad p \geq 0, \quad g\,p = 0$,
  where $g(x, y)$ is the gap between surfaces,
  $p = -\underline{n} \cdot \underline{\underline{\sigma}} \cdot \underline{n}$ is the contact pressure.

Methods

- Finite element method

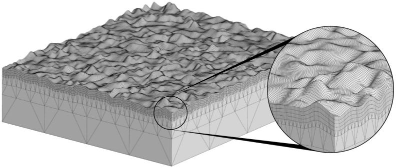

[1] Yastrebov, Wiley/ISTE (2013)

- Boundary element method

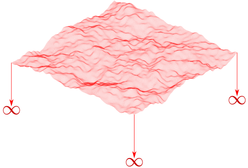

[2] Stanley & Kato, J Tribol 119 (1997)

Mapping

Problem mapping

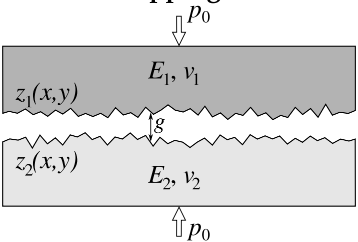

- **Flat** elastic[1] half-space with $E^* = \dfrac{E_1 E_2}{E_2(1-\nu_1^2) + E_1(1-\nu_2^2)}$
- **Rough** rigid[1] surface with $z^* = z_2 - z_1$
- Optimization problem[2]: $\min \mathcal{F}$

  under constraints $p \geq 0$ and $\frac{1}{A_0}\int\limits_A p dA = p_0$,

  with $\mathcal{F} = \int\limits_A p[u_z/2 + g]dA$

[1] Barber, Bounds on the electrical resistance between contacting elastic rough bodies, PRSL A 459 (2003)
[2] Kalker, Variational Principles of Contact Elastostatics, J Inst Maths Applics (1977)

Problem mapping

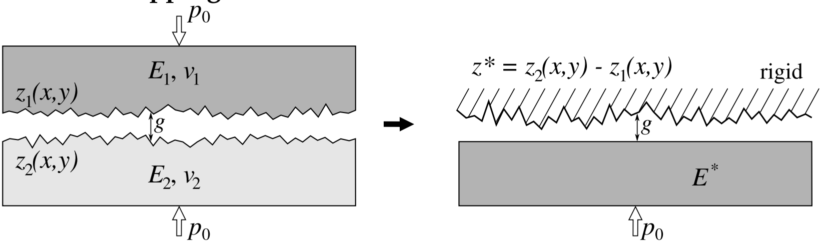

- **Flat** elastic[1] half-space with $E^* = \dfrac{E_1 E_2}{E_2(1-\nu_1^2) + E_1(1-\nu_2^2)}$
- **Rough** rigid[1] surface with $z^* = z_2 - z_1$
- Optimization problem[2]: $\min \mathcal{F}$

  under constraints $p \geq 0$ and $\frac{1}{A_0} \int\limits_A p dA = p_0$,

  with $\mathcal{F} = \int\limits_A p[u_z/2 + g] dA$

[1] Barber, Bounds on the electrical resistance between contacting elastic rough bodies, PRSL A 459 (2003)
[2] Kalker, Variational Principles of Contact Elastostatics, J Inst Maths Applics (1977)

Analytical models

Asperity based models

[1] Greenwood, Williamson. *P Roy Soc Lond A Mat* (1966)
[2] Bush, Gibson, Thomas. *Wear* (1975)
[3] Mc Cool. *Wear* (1986)
[4] Thomas. *Rough Surfaces* (1999)
[5] Greenwood. *Wear* (2006)
[6] Carbone. *J. Mech. Phys. Solids* (2009)
[7] Ciavarella, Greenwood, Paggi. *Wear* (2008)

Persson's model

[8] Persson. *J. Chem. Phys.* (2001)
[9] Persson. *Phys. Rev. Lett.* (2001)
[10] Persson, Bucher, Chiaia. *Phys. Rev. B* (2002)
[11] Müser. *Phys. Rev. Lett.* (2008)

Cross-link studies

[12] Manners, Greenwood. *Wear* (2006)
[13] Carbone, Bottiglione. *J. Mech. Phys. Solids* (2008)
[14] Paggi, Ciavarella. *Wear* (2010)

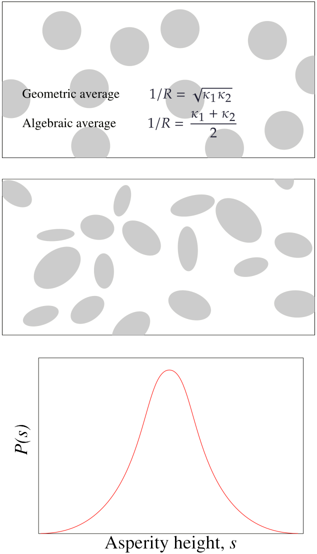

Fig. Asperity based models

Analytical models

Asperity based models

[1] Greenwood, Williamson. *P Roy Soc Lond A Mat* (1966)
[2] Bush, Gibson, Thomas. *Wear* (1975)
[3] Mc Cool. *Wear* (1986)
[4] Thomas. *Rough Surfaces* (1999)
[5] Greenwood. *Wear* (2006)
[6] Carbone. *J. Mech. Phys. Solids* (2009)
[7] Ciavarella, Greenwood, Paggi. *Wear* (2008)

Persson's model

[8] Persson. *J. Chem. Phys.* (2001)
[9] Persson. *Phys. Rev. Lett.* (2001)
[10] Persson, Bucher, Chiaia. *Phys. Rev. B* (2002)
[11] Müser. *Phys. Rev. Lett.* (2008)

Cross-link studies

[12] Manners, Greenwood. *Wear* (2006)
[13] Carbone, Bottiglione. *J. Mech. Phys. Solids* (2008)
[14] Paggi, Ciavarella. *Wear* (2010)

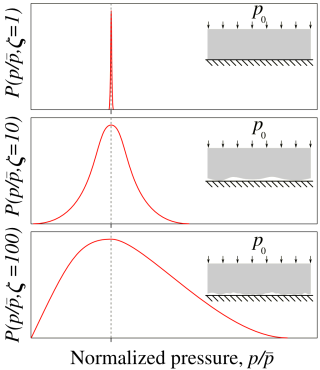

Fig. Persson's model

$$\boxed{\frac{\partial P(p,\zeta)}{\partial V(\zeta)} = \frac{1}{2}\frac{\partial^2 P(p,\zeta)}{\partial p^2}} \qquad P(0,\zeta) = 0$$

$$V(\zeta) = \tfrac{1}{2}E^* m_2(\zeta) = \frac{\pi E^*}{2}\int\limits_{k_l}^{\zeta k_l} k^3 \Phi^p(k)dk$$

Comparison of models

Asperity based models **Persson's model**

1. Evolution of the real contact area $A(p_0)$ for $A/A_0 \to 0$

$$\boxed{\frac{A}{A_0} = \frac{\kappa}{\sqrt{\langle|\nabla z|^2\rangle}}\frac{p_0}{E^*}}$$

$\kappa_{BGT} = \sqrt{2\pi} \approx 2.5$ *according to* [2-5]

$\kappa_P = \sqrt{8/\pi} \approx 1.6$ *according to* [6-7]

2. Evolution of the real contact area $A(p_0)$ for $\forall A/A_0$

$\frac{A}{A_0} = A(p_0, \alpha)/A_0$ *according to* [2-5]

$\frac{A}{A_0} = \mathrm{erf}\left(\sqrt{\frac{2}{\langle|\nabla z|^2\rangle}}\frac{p_0}{E^*}\right)$ *according to* [6-7]

[1] Greenwood, Williamson, P Roy Soc Lond A Mat 295 (1966)

[2] Bush, Gibson, Thomas, Wear 35 (1975)

[3] Mc Cool, Wear 107 (1986)

[4] Thomas, Rough Surfaces (1999)

[5] Greenwood, Wear 261 (2006)

[6] Persson, J. Chem. Phys. 115 (2001)

[7] Persson, Phys. Rev. Lett. 87 (2001)

[8] Persson, Bucher, Chiaia, Phys. Rev. B 65 (2002)

[9] Müser, Phys. Rev. Lett. 100, (2008)

Simulations set-up

- Cut-off parameters: $L/\lambda_l \otimes L/\lambda_s = \{1, 2, 4, 8, 16\} \otimes \{32, 64, 128, 256, 512\}$
- Hurst exponent $H = \{0.4, 0.8\}$
- 10 random surface realizations per combination of parameters
- Discretization: $\{L/\Delta x\} \times \{L/\Delta x\} = 2048 \times 2048$
- Search for contact area A', gap field $g(x, y)$ and gap PDF $P(g)$

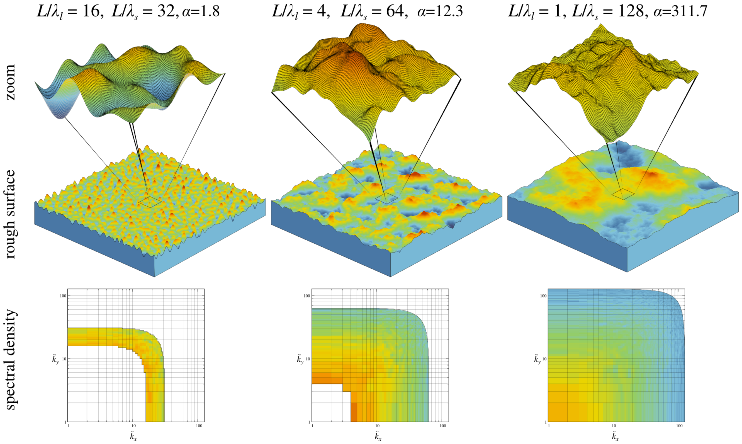

Contact area and contact pressure evolution

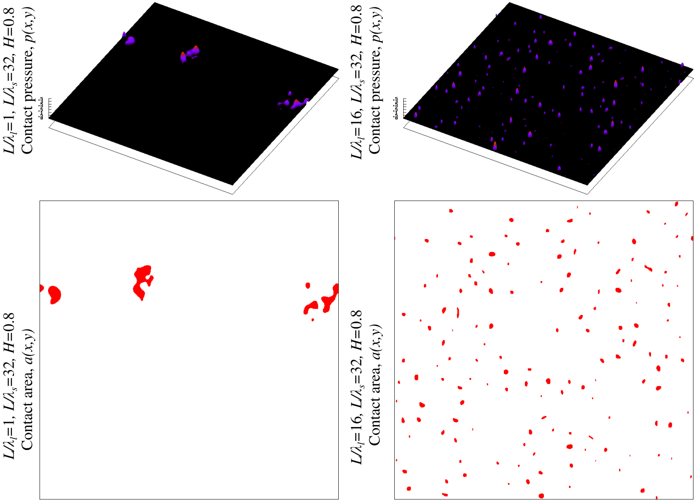

Contact area and contact pressure evolution

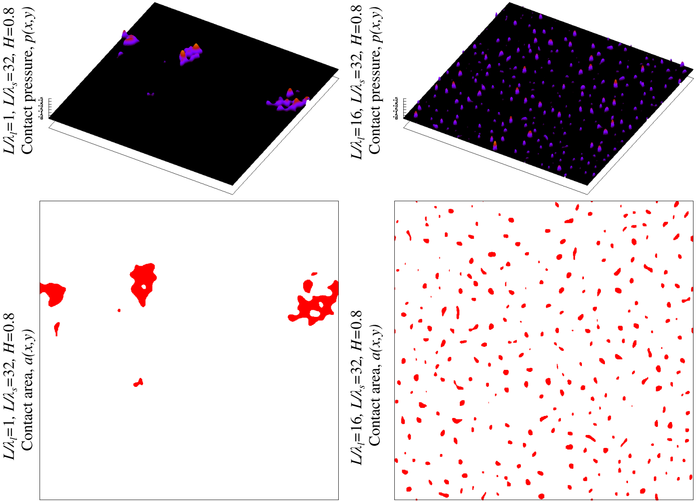

Contact area and contact pressure evolution

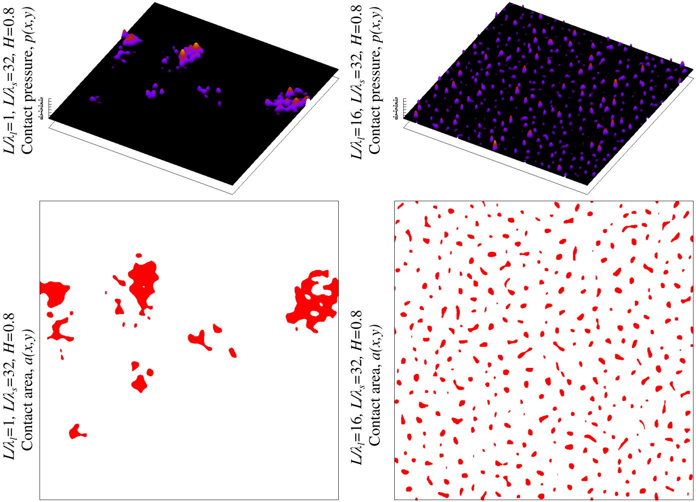

Contact area and contact pressure evolution

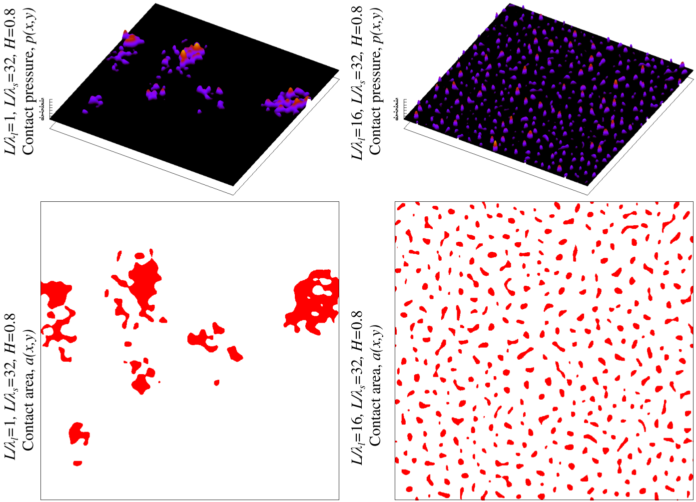

Contact area and contact pressure evolution

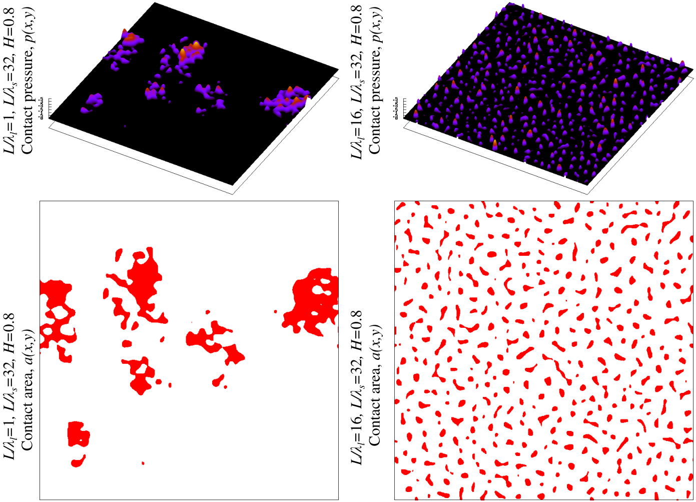

Contact area and contact pressure evolution

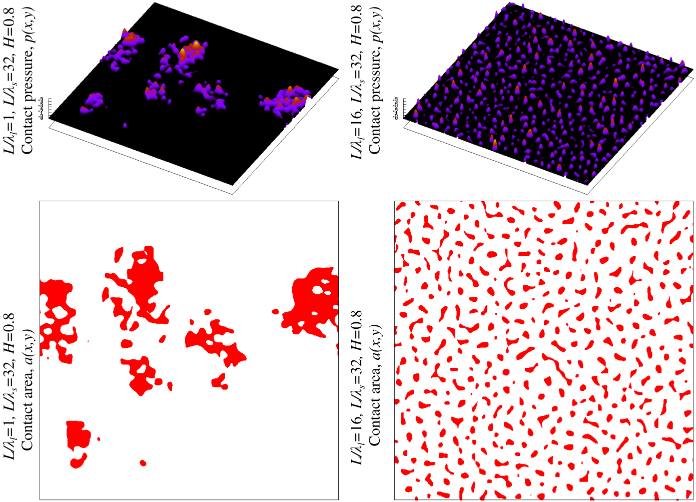

Contact area and contact pressure evolution

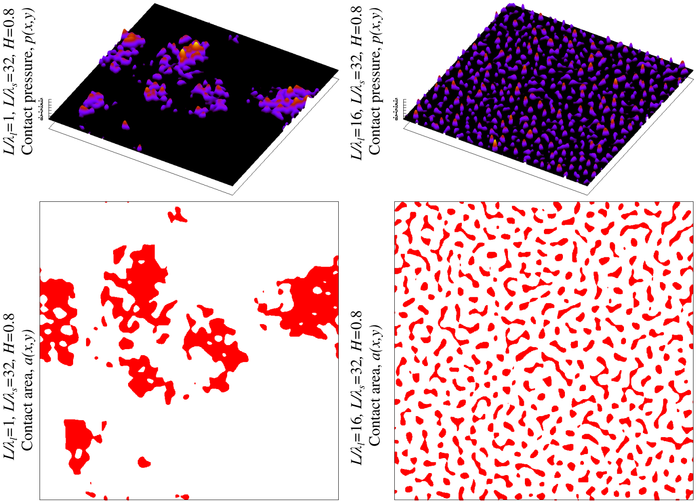

Contact area and contact pressure evolution

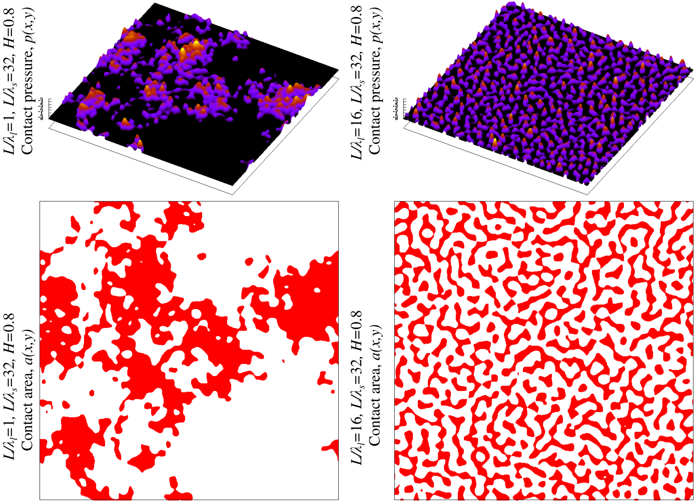

Contact area and contact pressure evolution

L/λ_l=1, L/λ_s=32, H=0.8
Contact pressure, $p(x,y)$

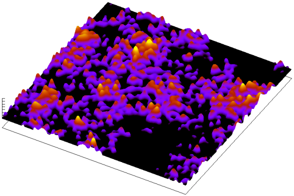

L/λ_l=16, L/λ_s=32, H=0.8
Contact pressure, $p(x,y)$

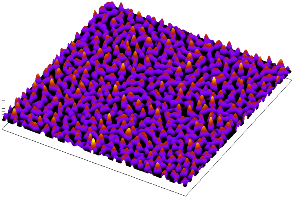

L/λ_l=1, L/λ_s=32, H=0.8
Contact area, $a(x,y)$

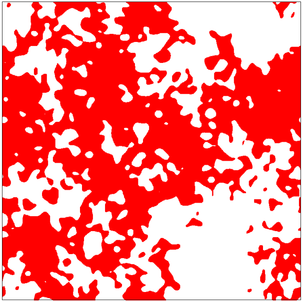

L/λ_l=16, L/λ_s=32, H=0.8
Contact area, $a(x,y)$

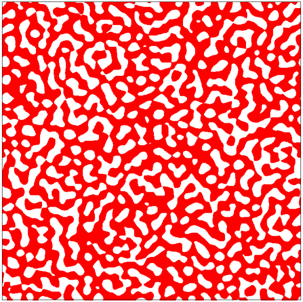

Contact area and contact pressure evolution

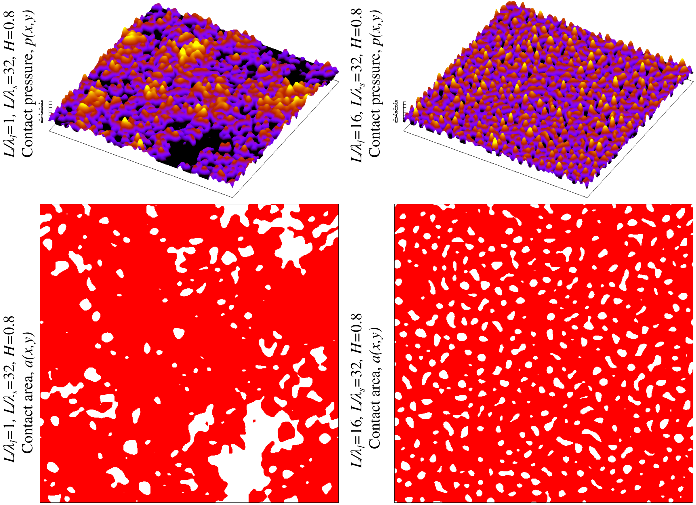

Contact area and contact pressure evolution

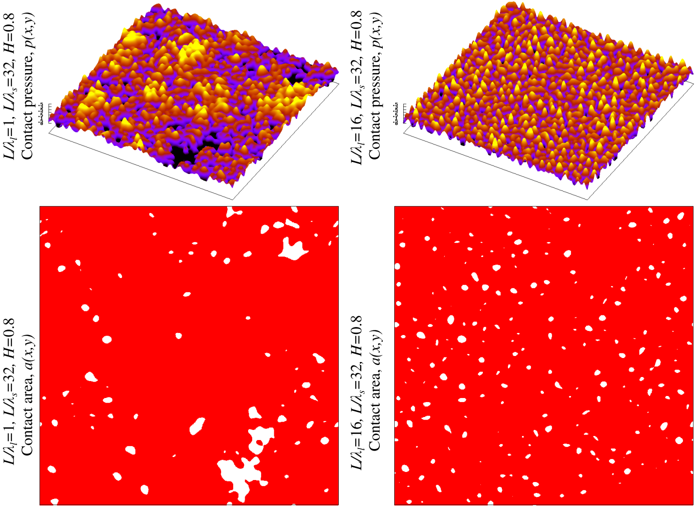

Contact area and contact pressure evolution

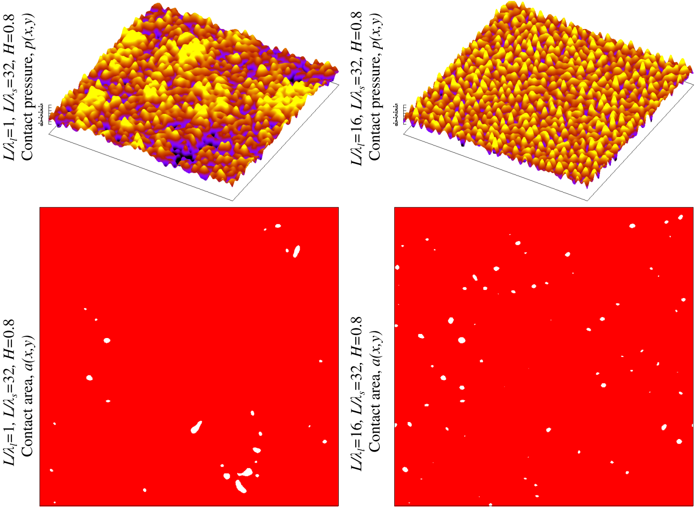

Contact area and contact pressure evolution

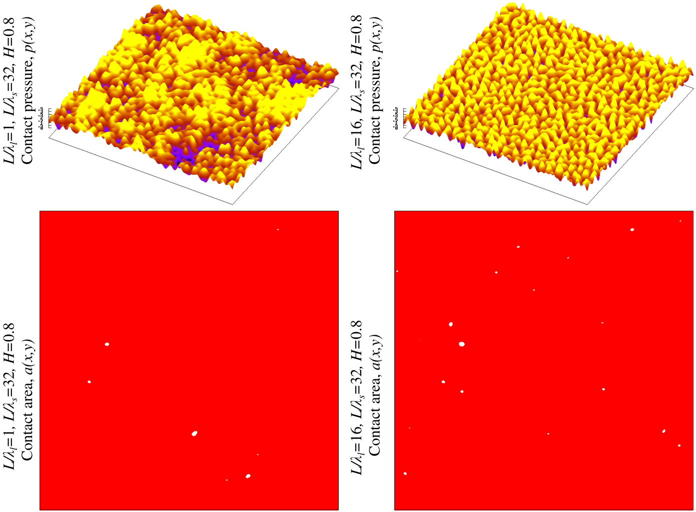

Contact area and contact pressure evolution

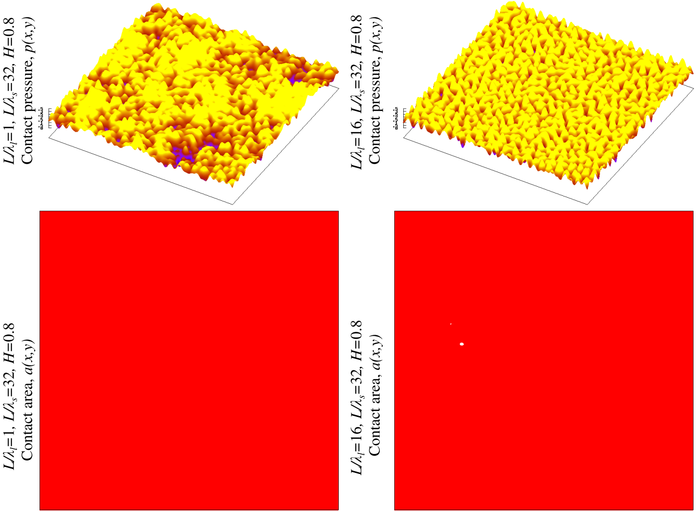

Results: contact area

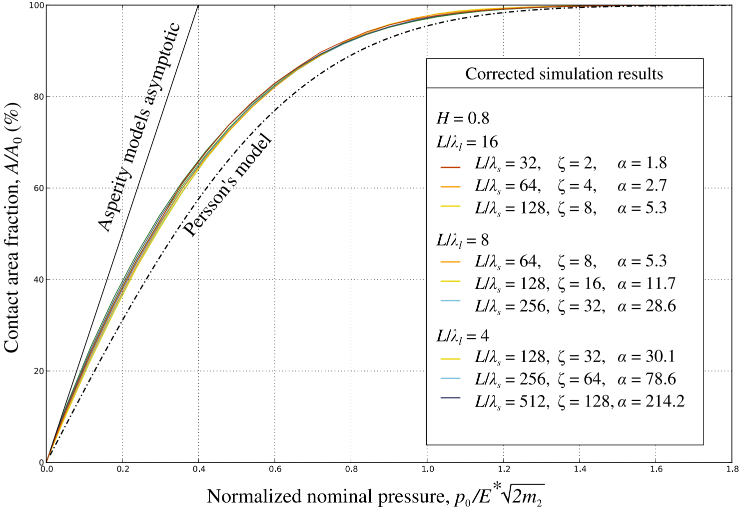

Multi-asperity models asymptotic[1,2], Persson's model[3]

[1] Bush, Gibson, Thomas, Wear 35 (1975), [2] Carbone, Bottiglione. *J. Mech. Phys. Solids* (2008), [3] Persson. *J. Chem. Phys.* (2001)

Results: contact area

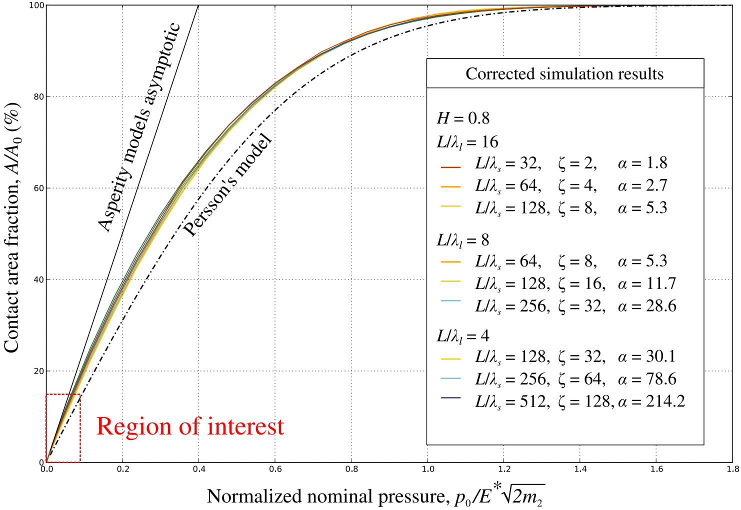

Multi-asperity models asymptotic[1,2], Persson's model[3]

[1] Bush, Gibson, Thomas, Wear 35 (1975), [2] Carbone, Bottiglione. *J. Mech. Phys. Solids* (2008), [3] Persson. *J. Chem. Phys.* (2001)

Results: contact area

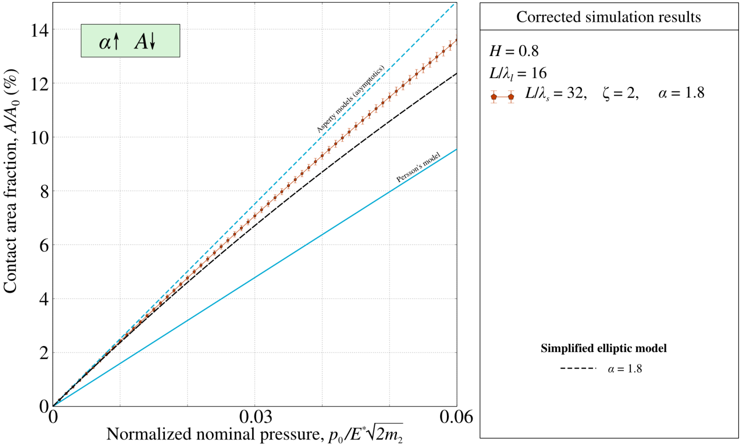

Simulations VS analytical models: Persson's model[1] and simplified elliptic model[2]

[1] Persson. *J. Chem. Phys.* (2001), [2] Greenwood. *Wear* (2006)

Results: contact area

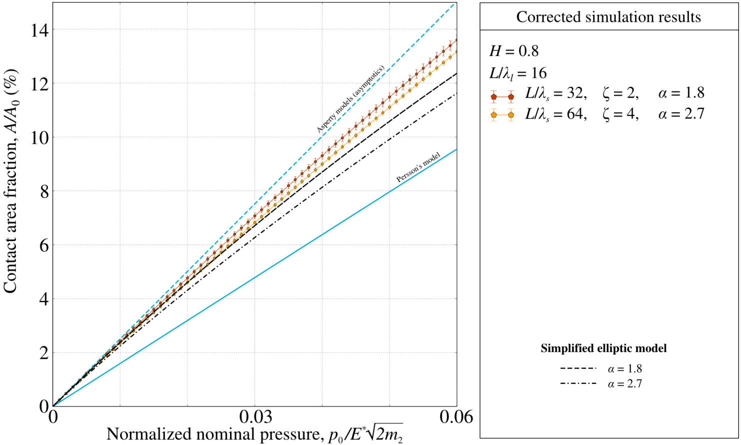

Simulations VS analytical models: Persson's model[1] and simplified elliptic model[2]

[1] Persson. *J. Chem. Phys.* (2001), [2] Greenwood. *Wear* (2006)

Results: contact area

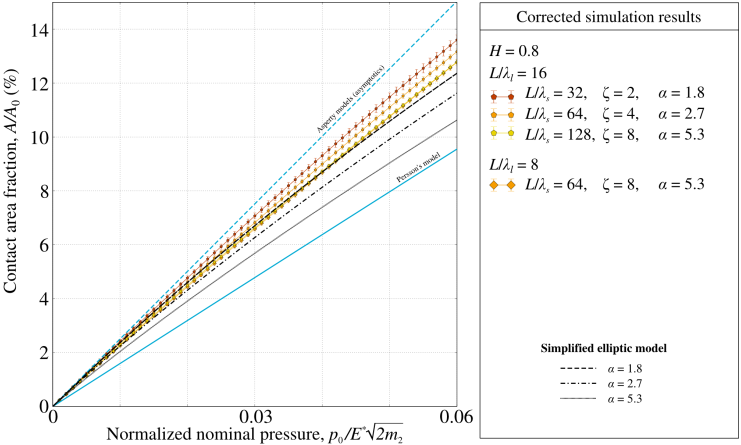

Simulations VS analytical models: Persson's model[1] and simplified elliptic model[2]

[1] Persson. *J. Chem. Phys.* (2001), [2] Greenwood. *Wear* (2006)

Results: contact area

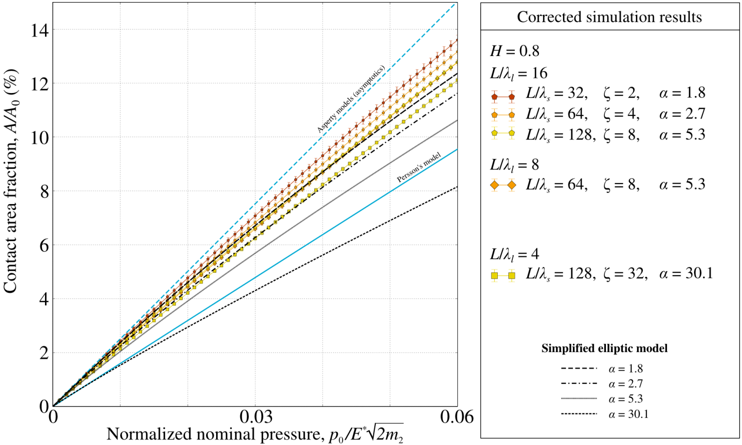

Simulations VS analytical models: Persson's model[1] and simplified elliptic model[2]

[1] Persson. *J. Chem. Phys.* (2001), [2] Greenwood. *Wear* (2006)

Results: contact area

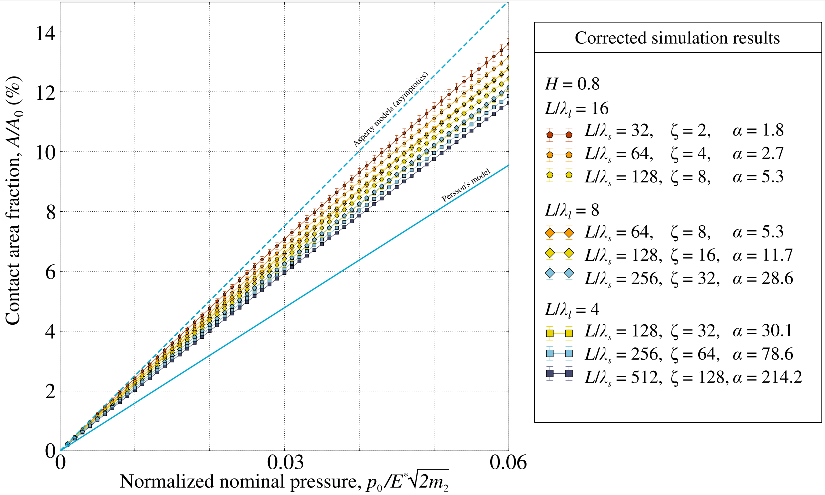

Corrected contact area (discretization independent): "magic" formula[1,2]

$$A_* \approx A_{\text{sim}} - \frac{\pi-1+\ln 2}{24} S_d \Delta x,$$

where S_d is the integral **perimeter** of the contact zones.

[1] Yastrebov, Anciaux, Molinari, *Tribol. Int.* 114 (2017)
[2] Yastrebov, Anciaux, Molinari, *J Mech Phys Solids* 107 (2017)

Results: contact area

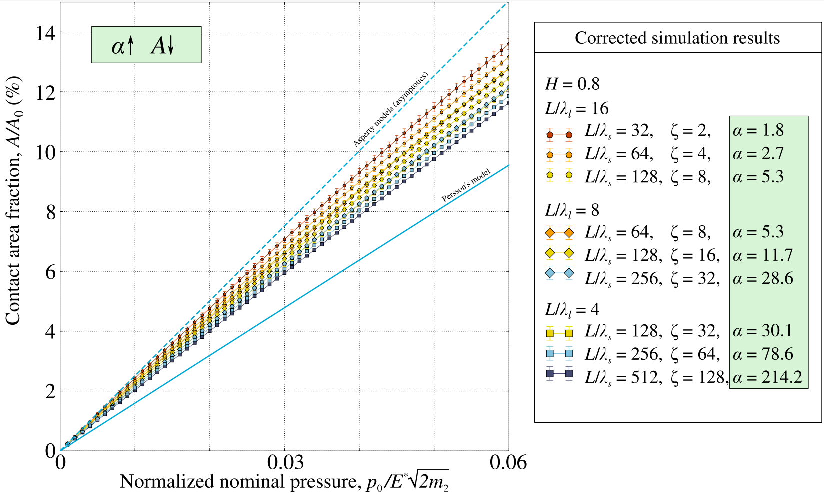

Corrected contact area (discretization independent): "magic" formula[1,2]

$$A_* \approx A_{\text{sim}} - \frac{\pi-1+\ln 2}{24} S_d \Delta x,$$

where S_d is the integral **perimeter** of the contact zones.

[1] Yastrebov, Anciaux, Molinari, *Tribol. Int.* 114 (2017)
[2] Yastrebov, Anciaux, Molinari, *J Mech Phys Solids* 107 (2017)

Numerical error correction

- Contact area is overestimated in simulations:

  $A_{\text{sim}} > A_*$

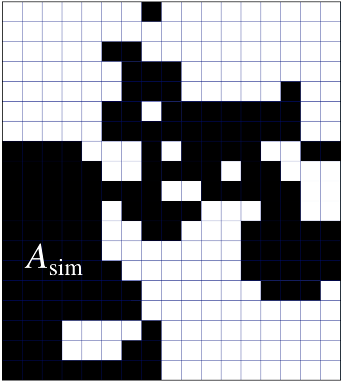

Numerical error correction

- Contact area is overestimated in simulations:

$$A_{\text{sim}} > A_*$$

- The overestimation is localized at boundary nodes:

$$A_{\text{sim}} > A_* > A^{\text{int}}_{\text{sim}}$$

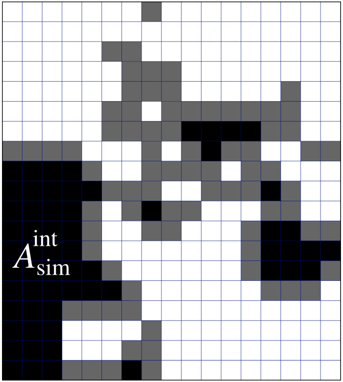

Numerical error correction

- Contact area is overestimated in simulations:

$$A_{\text{sim}} > A_*$$

- The overestimation is localized at boundary nodes:

$$A_{\text{sim}} > A_* > A_{\text{sim}}^{\text{int}}$$

- Boundary area ∼ perimeter S_d:

$$A_{\text{sim}} - A_{\text{sim}}^{\text{int}} = S_d \Delta x$$

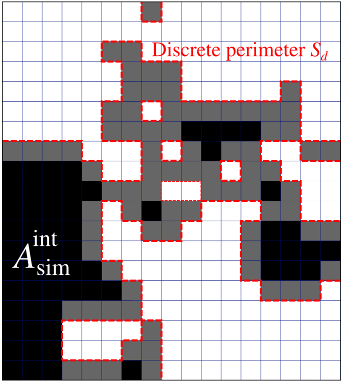

Numerical error correction

- Contact area is overestimated in simulations:

  $$A_{\text{sim}} > A_*$$

- The overestimation is localized at boundary nodes:

  $$A_{\text{sim}} > A_* > A_{\text{sim}}^{\text{int}}$$

- Boundary area ~ perimeter S_d:

  $$A_{\text{sim}} - A_{\text{sim}}^{\text{int}} = S_d \Delta x$$

- Manhattan S_d vs Euclidean metric S:

  $$\langle S \rangle = \frac{\pi}{4} \langle S_d \rangle$$

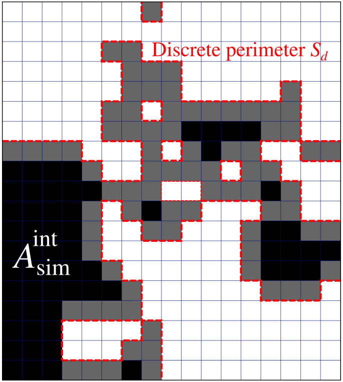

Numerical error correction

- Contact area is overestimated in simulations:

$$A_{\text{sim}} > A_*$$

- The overestimation is localized at boundary nodes:

$$A_{\text{sim}} > A_* > A_{\text{sim}}^{\text{int}}$$

- Boundary area ~ perimeter S_d:

$$A_{\text{sim}} - A_{\text{sim}}^{\text{int}} = S_d \Delta x$$

- Manhattan S_d vs Euclidean metric S:

$$\langle S \rangle = \frac{\pi}{4} \langle S_d \rangle$$

- True contact area estimation:

$$\boxed{A_* \approx A_{\text{sim}} - \beta \frac{\pi}{4} S_d \Delta x}$$

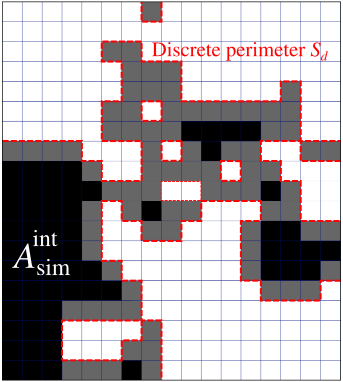

Numerical error correction: corrective factor

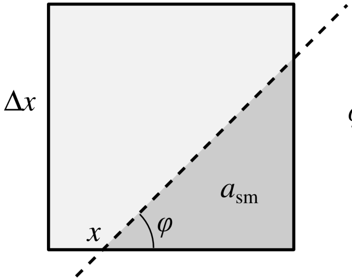

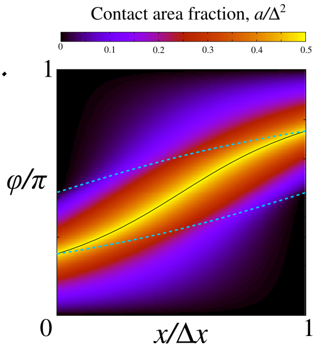

Corrective factor $\beta = \dfrac{\langle a_{\rm sm}\rangle}{\Delta x^2} = \dfrac{1}{\Delta x^2}\displaystyle\int\limits_0^h\int\limits_0^\pi a_{\rm sm}P(x,\phi)\,dx d\phi = \dfrac{\pi - 1 + \ln 2}{6\pi}$

$\beta = 0.15038761899481015 1606955\ldots$

True area estimation: $\boxed{A_* \approx A_{\rm sim} - \dfrac{\pi - 1 + \ln 2}{24} S_d \Delta x}$

Numerical error correction: convergence study

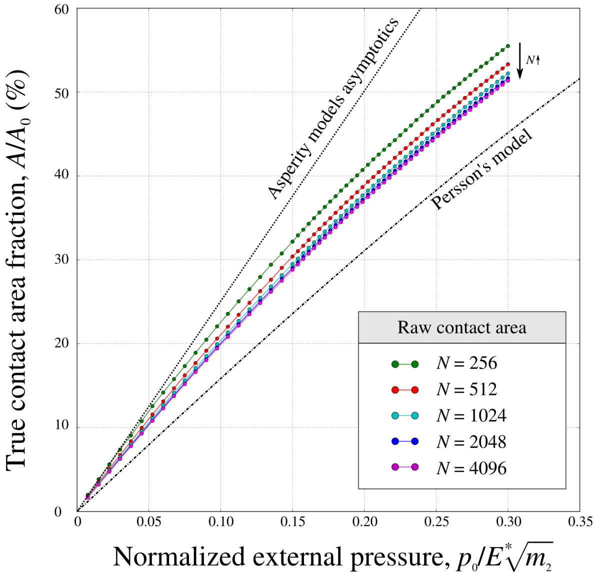

[1] Yastrebov, Anciaux, Molinari, Tribol Int 114 (2017)

Numerical error correction: convergence study

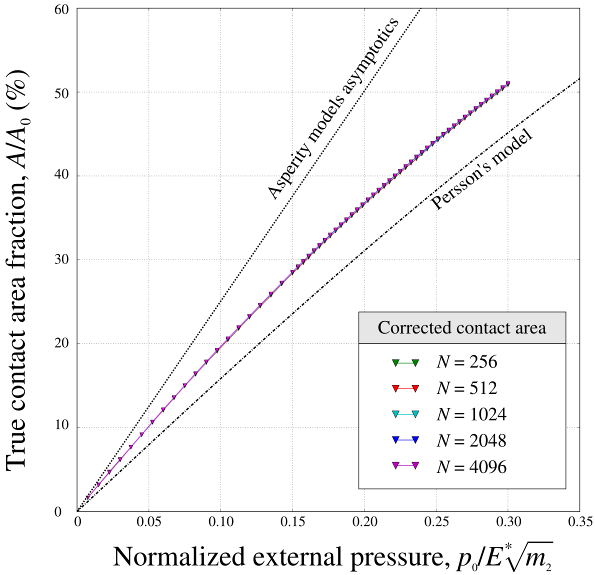

[1] Yastrebov, Anciaux, Molinari, Tribol Int 114 (2017)

Morphological correction

- Morphology of contact clusters

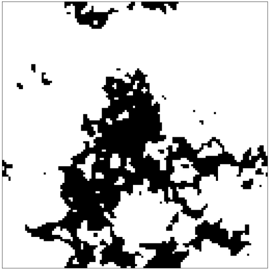

N=128, raw

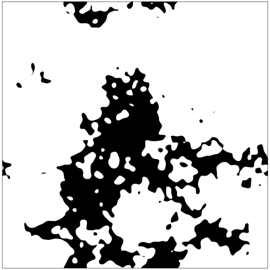

N=2048, raw

- Morphology of contact clusters

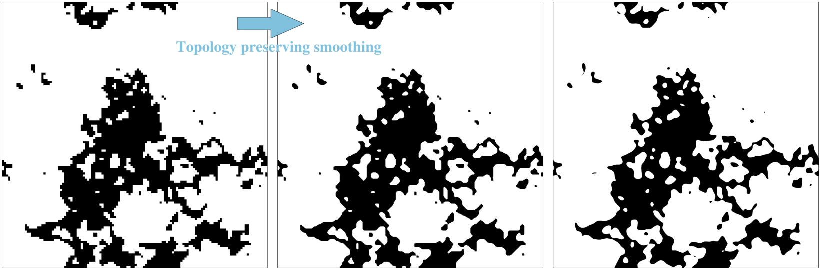

N=128, raw N=128, smoothed N=2048, raw

Topologically preserving smoothing results in realistic cluster geometry

[1] Couprie & Bertrand, *J Electr Imag* 13 (2004)

Real contact area: accurately computed

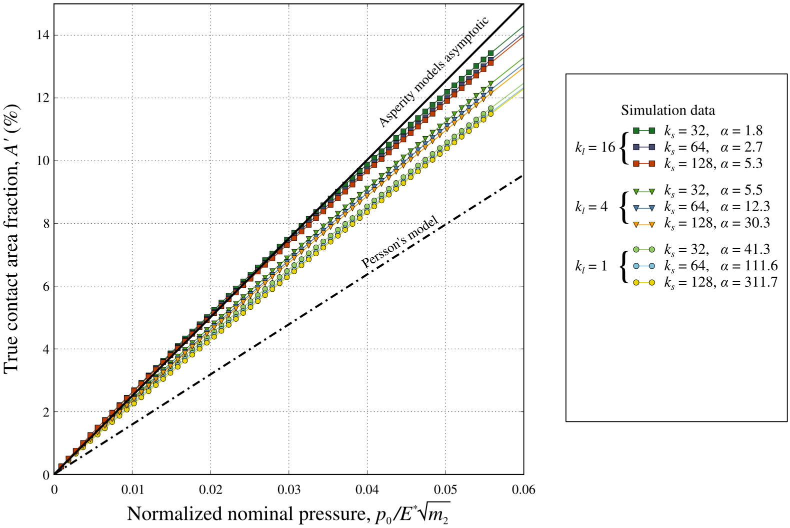

Raw data

[1] Yastrebov, Anciaux, Molinari, Int J Solids Struct 52 (2015)

Real contact area: accurately computed

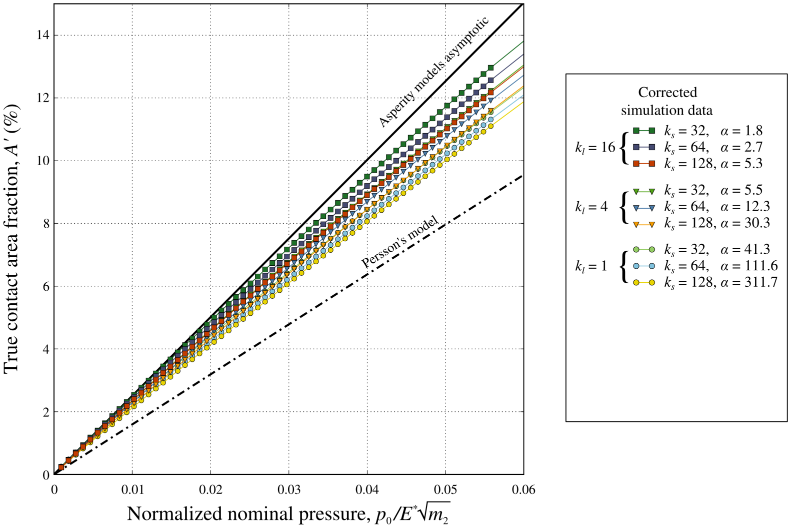

Corrected data

[2] Yastrebov, Anciaux, Molinari, *J Mech Phys Solids* 107 (2017)

Real contact area: accurately computed

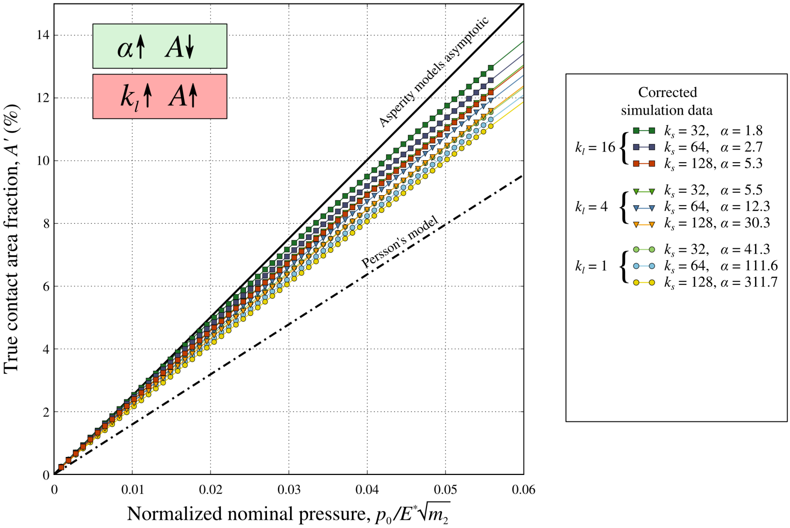

Corrected data

[2] Yastrebov, Anciaux, Molinari, *J Mech Phys Solids* 107 (2017)

Real contact area: accurately computed

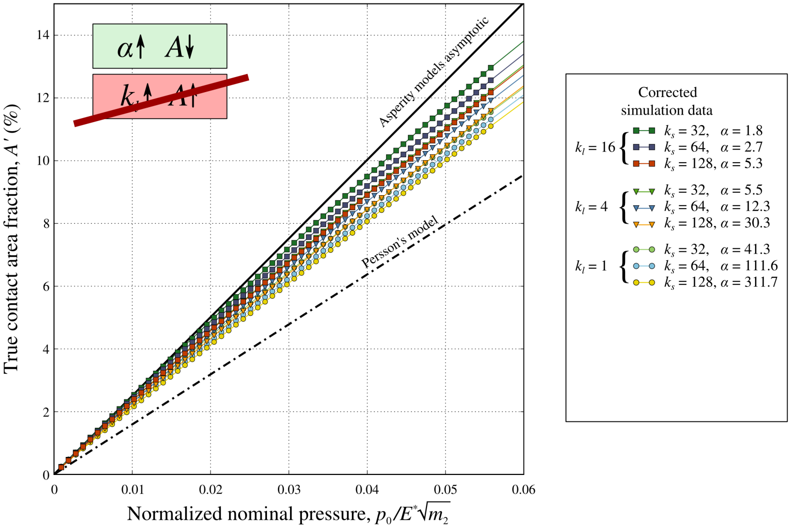

Corrected data

[2] Yastrebov, Anciaux, Molinari, *J Mech Phys Solids* 107 (2017)

Role of Nayak parameter α

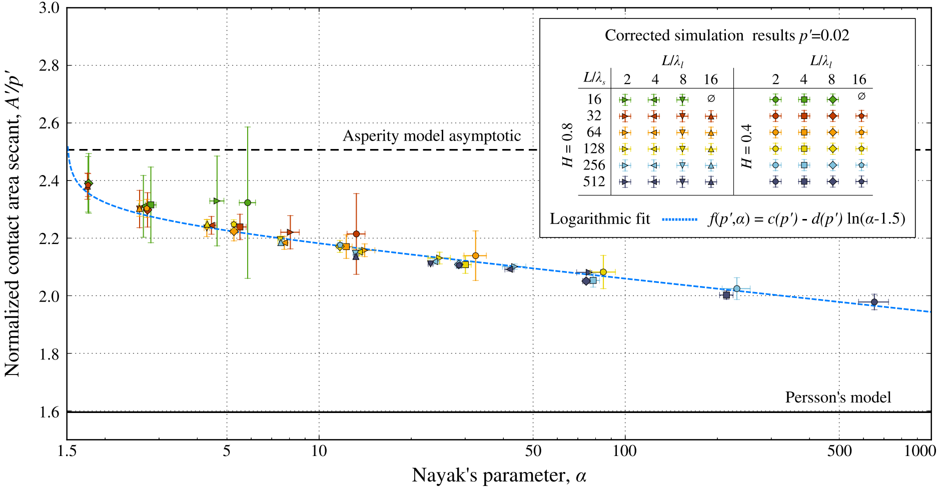

Numerical results: [1] Yastrebov, Anciaux, Molinari, J Mech Phys Solids 107 (2017)

Role of Nayak parameter α

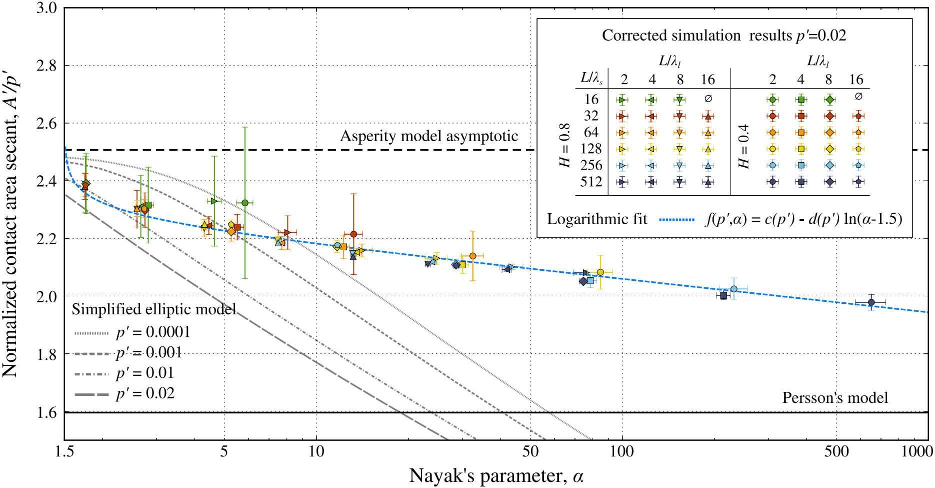

Numerical results: [1] Yastrebov, Anciaux, Molinari, J Mech Phys Solids 107 (2017)

Simplified elliptic model: [2] Greenwood, Wear (2006)

Role of Nayak parameter α

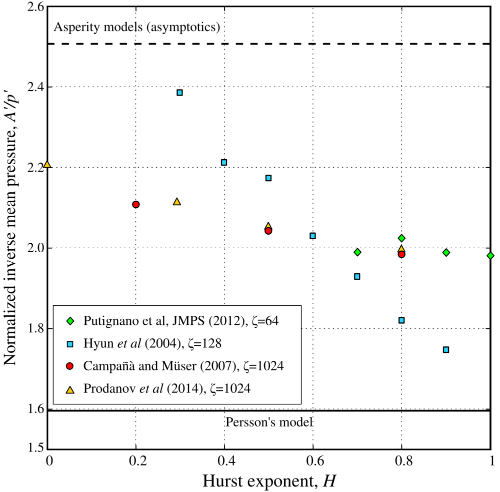

Comparison with other numerical studies
Nayak-Hurst relationship

$$\alpha(H,\zeta) = \frac{3}{2}\frac{(1-H)^2}{H(H-2)}\frac{(\zeta^{-2H}-1)(\zeta^{4-2H}-1)}{(\zeta^{2-2H}-1)^2}$$

Role of Nayak parameter α

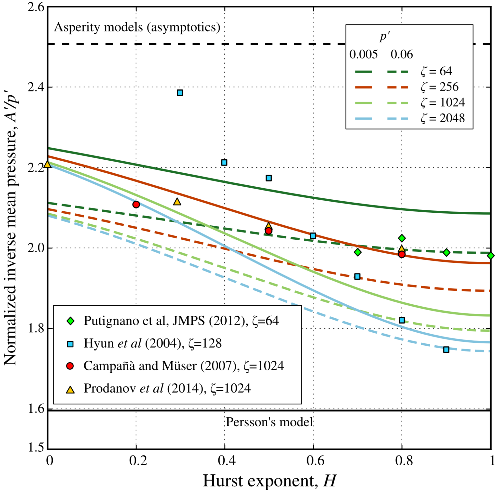

Comparison with other numerical studies
Nayak-Hurst relationship

$$\alpha(H,\zeta) = \frac{3}{2}\,\frac{(1-H)^2}{H(H-2)}\,\frac{(\zeta^{-2H}-1)(\zeta^{4-2H}-1)}{(\zeta^{2-2H}-1)^2}$$

Phenomenological relationship

- Contact area A grows with applied pressure p_0 as

$$\frac{A}{A_0} = a(\alpha)\frac{p_0}{E^*\sqrt{2m_2}} - b(\alpha)\left[\frac{p_0}{E^*\sqrt{2m_2}}\right]^2$$

- Contact area fraction $A' = A/A_0$ grows with normalized applied pressure $p' = p_0/E^*\sqrt{2m_2}$

$$\boxed{A' = a(\alpha)p' - b(\alpha)p'^2}$$

- With ≈universal adimensional constants:

$$a(\alpha) = 2.35 - 0.057\ln(\alpha - 1.5)$$

$$b(\alpha) = 2.85 - 0.24\ln(\alpha - 1.5)$$

- Pressure dependent friction coefficient:

$$\mu(p') = \mu_0\left[1 - \frac{b(\alpha)}{a(\alpha)}p'\right]$$

with $\mu_0 = a(\alpha)\tau_{max}/E^*\sqrt{2m_2}$,
τ_{max} is the maximum shear traction the contact interface can bear.

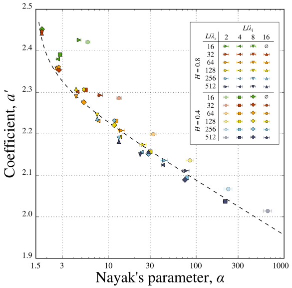

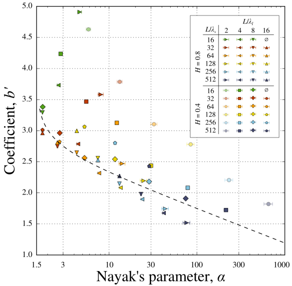

Conclusions

- Contact area depends weakly on Nayak parameter $\alpha = m_0 m_4 / m_2^2$

$$\boxed{A' = a(\alpha)p' - b(\alpha)p'^2}$$

with $a(\alpha) = 2.35 - 0.057\ln(\alpha - 1.5)$, $\quad b(\alpha) = 2.85 - 0.24\ln(\alpha - 1.5)$

- No effect of fractal dimension D_f *per se* on the contact area
it affects the contact area only through the Nayak parameter
- Using the area correction technique we could go to magnifications up to 600

$$\zeta = \frac{\lambda_l}{\lambda_s} = \frac{k_s}{k_l} = \frac{q_2}{q_1} < 600$$

- Need a wider interval of Nayak parameter to be studied
May be there is a hidden dependence on the fractal dimension?

☺ Thank you for your attention!